

Reactions of Peroxyacetyl Radicals with Reduced Sulfur Compounds

Gerassimos Mineshos¹, Sotirios Glavas^{1,*}, and Ulrich Schurath²

¹ Department of Chemistry, University of Patras, GR-26110 Patras, Greece

² Institut für Physikalische Chemie, Universität Bonn, D-W-5300 Bonn,
Federal Republic of Germany

Summary. The reaction of peroxyacetyl radicals with reduced sulfur compounds was studied at 55°C in N₂ at 1 000 mbar total pressure. The radicals were generated in equilibrium with peroxyacetyl nitrate and NO₂ in large excess. The pseudo first order decay of *PAN* was measured in the absence and presence of several 100 ppm CH₃SH, C₂H₅SH, *n*-C₄H₉SH, (CH₃)₂S, and (CH₃S)₂. Computer simulations yielded the following rate constants of peroxyacetyl radicals with the above mentioned sulfur compounds: 3.7, 2.8, 13.0, 0.9, and 1.8·10⁻¹⁶ cm³/s, respectively. An electron capturing compound of the thiols with NO₂ was observed.

Keywords. Reactions; *PAN*; Sulfur compounds.

Reaktionen von Peroxyacetylradikalen mit reduzierten Schwefelverbindungen

Zusammenfassung. Die Reaktionen von Peroxyacetylradikalen mit reduzierten Schwefelverbindungen wurden bei 55°C in NO₂ bei einem Totaldruck von 1 000 mbar untersucht. Die Radikale wurden im Gleichgewicht mit Peroxyacetylnitrat und NO₂ in großem Überschuß generiert. Der nach erster Ordnung verlaufende Zerfall von *PAN* wurde in Abwesenheit und Anwesenheit und von einigen ppm CH₃SH, C₂H₅SH, *n*-C₄H₉SH, (CH₃)₂S und (CH₃S)₂ gemessen. Computersimulierung der Geschwindigkeitskonstanten für die Peroxyacetylradikale ergab mit den genannten Schwefelverbindungen 3.7, 2.8, 13.0, 0.9 und 1.8·10⁻¹⁶ ch³/s. Eine elektronenfangende Verbindung der Thiole mit NO₂ wurde beobachtet.

Introduction

NO₂ is a unique photochemical precursor of ozone in the troposphere. The partitioning of total odd nitrogen between NO₂ and photochemically inactivated transient reservoir species such as *PAN* in the atmosphere is determined (a) by the strongly temperature-dependent reversible dissociation of *PAN* into NO₂ and CH₃COO₂ and (b) by secondary reactions of the peroxyacetyl radicals with NO and other possible substrates. Extremely slow reactions of *PAN* with various trace gases including SO₂ have been studied by Pate et al. [1] before the radical mechanism of these reactions was definitely established [2]. A study of CH₃COO₂ radical reactions with various olefins, which took advantage of the correct mechanism,

has been reported [3]. In the present work we report an analogous study of peroxyacetyl reactions with reduced sulfur compounds which are known to be emitted by natural sources. In particular the emissions of dimethyl sulfide from the oceans constitute approximately half the natural global sulfur budget [4]. These reactions to the best of our knowledge have not been studied before.

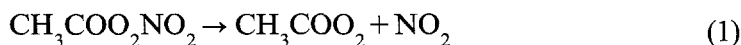
Experimental Part

All experiments were carried out in a 4.5 l cylindrical glass vessel equipped with two septum ports for sampling and a teflon stopcock for its connection to a vacuum line which in turn was provided with teflon stopcocks. The glass vessel was immersed in an oil bath maintained at a constant temperature of $55 \pm 0.5^\circ\text{C}$. The relatively high temperature is necessary so that *PAN* quickly dissociates into $\text{CH}_3\text{COO}_2 + \text{NO}_2$ and thus reaction (1) is not the rate limiting one. To avoid the fast destruction of *PAN* we added NO_2 which shifts reaction (1) to the left via reaction (-1) and thus extends the lifetime of *PAN* sufficiently to carry out our experiments. Nitrogen (99.99%) at 1 000 mbar was always used as the matrix atmosphere and not air, in order to avoid interferences from the air peak on the ECD used for the monitoring of *PAN* and the other electron capturing compounds. However, according to carrier gas manufacturers 5 ppm oxygen are expected to be present as impurity of nitrogen. It must be pointed out that the total oxygen concentration in our experiments results from the above mentioned 5 ppm plus 20 ppm which are contained in NO_2 from its preparation, thus making a total oxygen of 25 ppm; this value was also used in the simulations. Samples were withdrawn with a gas tight syringe and injected into a Shimadzu GC equipped with an electron capturing detector. The analytical column used was made of glass, 60 cm long, 3 mm i. d., packed with 4.8% QF-1 + 0.18% diglycerol on Chromosorb G-AW-DMCS (80-100 mesh). The *PAN* peak eluted in 3.3 minutes.

NO_2 was prepared daily by measuring 100 mbar NO (99.85%) and reacting it with extra pure grade O_2 to a total pressure of 1 000 mbar. The prepared NO_2 was found by chemiluminescence detection to contain 0.9% NO . Pure liquid *PAN* in tridecane was prepared according to the method of Gaffney et al. [5]. The appropriate amount of NO_2 was first introduced into the evacuated reaction vessel. Subsequently *PAN* in tridecane was injected into the gas handling system and its vapour was flushed into the reaction vessel as it was brought to 1 000 mbar total pressure with pure nitrogen. The final mixing ratios were 2.2 ppm NO_2 and typically 350-500 ppb *PAN*. The *PAN* concentration in the reaction vessel was analyzed every 15 minutes for approximately 80 minutes, in order to establish its slow decay rate. After this period gas and/or vapour mixtures in nitrogen of CH_3SH (99.5%), $\text{C}_2\text{H}_9\text{SH}$ (99%), $\text{C}_4\text{H}_9\text{SH}$ (99%), $(\text{CH}_3)_2\text{S}$ (99%) and $(\text{CH}_3\text{S})_2$ (99%), were injected into the reaction vessel, making the reduced sulfur compound concentration in the reaction vessel from 50-2 500 ppm. Mixing in the glass vessel was achieved by repeated pumping with the syringe. Separate measurements with a thermocouple showed that the process was isothermal. Analysis of *PAN* and other detectable products was continued until more than 90% of *PAN* was consumed.

Results and Discussion

To check our system, control experiments were first carried out with *PAN* in the presence of excess NO at 28°C in 1 000 mbar N_2 . The obtained first order plot was linear throughout and yielded a slope of $7 \cdot 10^{-4} \text{ s}^{-1}$. This value corresponds to the rate constant of reaction (1)

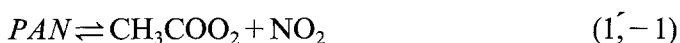


which is the rate limiting in the presence of excess NO and agrees with the previously reported values [2, 3, 6].

PAN in nitrogen gas containing 2.2 ppm NO_2 at 55°C decayed at a rate of only $(3.5 \pm 1) \cdot 10^{-5} \text{ s}^{-1}$, although the first order rate constant of reaction (1) at this temperature is known to be $2.4 \cdot 10^{-2} \text{ s}^{-1}$. The decay rate is reduced because reaction (1) is no longer rate determining in the presence of NO_2 .

The *PAN*- NO_2 - N_2 system was simulated by a 24 reaction mechanism listed in Table 1 using the Facsimile software. The rate constant of reaction (1) was obtained from the present study and is in agreement with the value of our recent study [6] using the Arrhenius parameters of Schurath and Vipprecht [3]. Most of the rate constants of Table 1 were obtained from the most recent literature survey available [7]. The rest of the rate constants were obtained from other recent references [8–12]. For reactions found in their fall off region at 1 Atm pressure at 55°C , the appropriate second order rate constants were calculated using Troe's expression. The literature rate constants were used as reported and no attempt was made to adjust them to our experimental data.

The fitting parameters in the simulations before the addition of the sulfur compounds were the wall decay rate constants of *PAN* and CH_3COO_2 radicals. The resulting values were $4 \cdot 10^{-5}$ and 0.30 s^{-1} , respectively. These values are in good agreement with the respective values of $2 \cdot 10^{-5}$ and 0.40 s^{-1} obtained from Fig. 1. If we assume steady state conditions for the peroxyacetyl radicals in the following simplified reaction scheme:



we obtain the expression (A):

$$-d \ln[\text{PAN}]/dt = k_{21} + k_1 \cdot k_{22}/k_{-1} [\text{NO}_2]. \quad (\text{A})$$

The plot $-d \ln[\text{PAN}]/dt$ vs. $[\text{NO}_2]^{-1}$, shown in Fig. 1, is linear. Its intercept yields k_{21} , while the slope, after substitution of k_1 and k_{-1} , yields k_{22} .

After the addition of the sulfur compound, the *PAN* decay increased as well as the formation of methyl nitrate. In order to account for the increased decay of

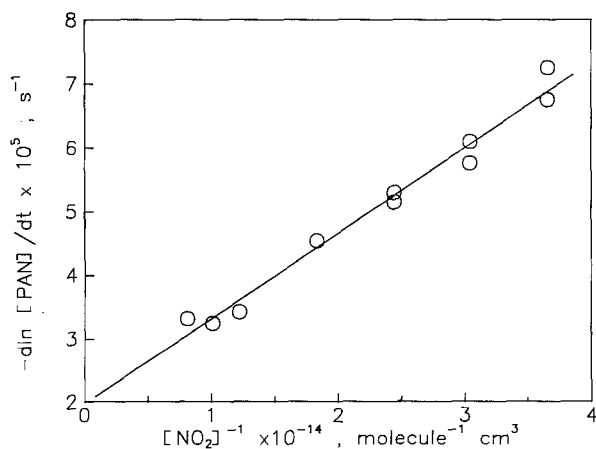


Fig. 1. Plot of first order decay rate constant of *PAN* vs. $1/[\text{NO}_2]$, cf. equation (A)

Table 1. Simulation mechanisms

Reaction No.	Reaction	Rate constants 55°C	Reference
1	$PAN \rightarrow CH_3COO_2 + NO_2$	$1.7 \cdot 10^{-2}$	[3, 5]
-1	$CH_3COO_2 + NO_2 \rightarrow PAN$	$7.0 \cdot 10^{-12}$	7
2	$2 CH_3COO_2 \rightarrow 2 CH_3 + 2 CO_2 + O_2$	$2.8 \cdot 10^{-12} \cdot 10^{230/T}$	7
3	$CH_3 + O_2 (+M) \rightarrow CH_3O_2$	$8.0 \cdot 10^{-13}$	7
4	$2 CH_3O_2 \rightarrow 2 CH_3O + O_2$	$1.2 \cdot 10^{-13}$	7
5	$2 CH_3O_2 \rightarrow HCHO + CH_3 + OH + O_2$	$2.0 \cdot 10^{-13}$	7
6	$2 CH_3O_2 \rightarrow CH_3OCH_3 + O_2$	$3.3 \cdot 10^{-14}$	7
7	$CH_3CO_3 + CH_3O_2 \rightarrow CH_3 + CO_2 + CH_3O + O_2$	$1.8 \cdot 10^{-9} \cdot 10^{-781/T}$	8
8	$CH_3CO_3 + CH_3O_2 \rightarrow CH_3CO_2H + HCHO + O_2$	$4.1 \cdot 10^{-15} \cdot 10^{912/T}$	8
9	$CH_3O + O_2 \rightarrow HCHO + HO_2$	$7.2 \cdot 10^{-14} \cdot 10^{-469/T}$	7
10	$CH_3CO_3 + HO_2 \rightarrow CH_3CO_3H + O_2$	$1.0 \cdot 10^{-13} \cdot 10^{577/T}$	9
11	$CH_3O + NO_2 \rightarrow CH_3ONO_2$	$1.4 \cdot 10^{-11}$	7
12	$CH_3O + NO_2 \rightarrow HCHO + HONO$	$1.5 \cdot 10^{-13}$	10
13	$CH_3 + NO_2 \rightarrow CH_3O + NO$	$2.5 \cdot 10^{-11}$	11
14	$HO_2 + NO \rightarrow NO_2 + OH$	$3.7 \cdot 10^{-12} \cdot 10^{104/T}$	7
15	$OH + NO_2 (+M) \rightarrow HONO_2$	$1.0 \cdot 10^{-11}$	7
16	$CH_3O_2 + HO_2 \rightarrow CH_3OOH + O_2$	$1.7 \cdot 10^{-13} \cdot 10^{434/T}$	7
17	$CH_3O_2 + NO \rightarrow CH_3O + NO_2$	$4.2 \cdot 10^{-12} \cdot 10^{78/T}$	7
18	$CH_3CO_3 + NO \rightarrow CH_3 + CO_2 + NO_2$	$1.4 \cdot 10^{-11}$	7
19	$CH_3O + NO \rightarrow CH_3ONO$	$1.9 \cdot 10^{-11}$	7
20	$CH_3O + NO \rightarrow HCHO + HNO$	$1.3 \cdot 10^{-12}$	12
21	$PAN + wall \rightarrow$	$4 \cdot 10^{-5}$	This work
22	$CH_3CO_3 + wall \rightarrow$	0.3	This work
23	$PAN + OH \rightarrow$ products	$1.7 \cdot 10^{-13}$	7
<i>B</i>			
24	$CH_3COO_2 + CH_3SH \rightarrow$ products	k_{24}	This work
25	$OH + CH_3SH \rightarrow$ products	$9.9 \cdot 10^{-12} \cdot 10^{156/T}$	13
26	$HO_2 + CH_3SH \rightarrow$ products	$6.0 \cdot 10^{-11}$	13
27	$CH_3S + NO \rightarrow CH_3SNO$	$1.8 \cdot 10^{-12} \cdot 10^{390/T}$	13
28	$CH_3S + NO_2 \rightarrow CH_3SNO_2$	$5.6 \cdot 10^{-11}$ (at 25 C)	13
29	$CH_3SH + NO_2 \rightarrow CH_3SNO + OH$	$3.2 \cdot 10^{-16} \cdot 10^{-1867/T}$	14
30	$CH_3SH + NO_2 \rightarrow CH_3SOH + NO$	$2.0 \cdot 10^{-9} \cdot 10^{-4472/T}$	[14]

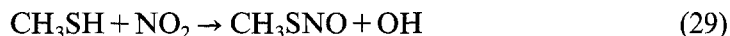
Units: $cm^3/mol \cdot s$ and s^{-1}

PAN after the addition of the sulfur compound, the mechanism of Table 1 was completed with part B dealing with the chemistry of the sulfur compounds. In Table 1 B the reactions for CH_3SH along with the respective rate constants obtained from Refs. [7, 13, 14] are given. The rate constants of the reactions of the rest of the reactants and their respective radicals are given in Table 2. When the required reaction rate constants are not available we employed the values given for CH_3SH . Although reactions 29 and 30 are very slow they have an important effect on *PAN* and CH_3ONO_2 profiles obtained in the simulations. It is reported that CH_3SH

Table 2. Rate constants employed in part *B* of reaction mechanisms at 25°C as well as those of the sulfur compounds with NO₃ radicals

	OH · 10 ¹¹	NO ₃ · 10 ¹³	NO ₂	NO	O ₂
CH ₃ SH	3.3 [7]	10 [17]	1.7 · 10 ⁻²² [14]	–	–
CH ₃ S	–	–	5.6 · 10 ⁻¹¹ [13]	2.5 · 10 ⁻¹¹ [15]	3 · 10 ⁻¹⁸ [13]
C ₂ H ₅ SH	4.7 [18]	12 [17]	–	–	–
C ₂ H ₅ S	–	–	9.2 · 10 ⁻¹¹ [16]	4.6 · 10 ⁻¹¹ [16]	<2 · 10 ⁻¹⁷ [16]
C ₄ H ₉ SH	4.4 [18]	–	–	–	–
(CH ₃) ₂ S	0.5 [13]	10 [17]	–	–	–
(CH ₃ S) ₂	20 [13]	5.3 [17]	–	–	–

reacts in the dark with NO₂ and yields several products among which are OH and NO, according to following equations [19].



Because OH and NO are known to react with *PAN* and CH₃COO₂, respectively, these reactions are also included in the reaction mechanism. The reported rate constant of the reaction CH₃SH + NO₂ is slow enough [14] to preclude the disappearance of NO₂ and thus the increased *PAN* decay, observed after the addition of the sulfur compound, cannot be attributed to the shift to the right of the *PAN* thermal decay reaction (1). This is corroborated by the simulation results, shown in Fig. 2, which indicate that NO₂ remained almost constant, if not slightly increased, throughout the experiment. The fitting parameter in this simulation was the rate constant of reaction *k*₂₄. Figure 2 shows the experimental points and the simulation results for one experiment of methane thiol.

Repeated simulations of six experiments for each sulfur compound under varied initial concentration yielded the results:

$$k_{24} = 3.7(\pm 0.4) \cdot 10^{-16} \text{ cm}^3/\text{s} \text{ for } \text{CH}_3\text{SH}$$

$$k_{24} = 2.8(\pm 0.4) \cdot 10^{-16} \text{ cm}^3/\text{s} \text{ for } \text{C}_2\text{H}_5\text{SH}$$

$$k_{24} = 13.0(\pm 1.3) \cdot 10^{-16} \text{ cm}^3/\text{s} \text{ for } \text{C}_4\text{H}_9\text{SH}$$

$$k_{24} = 0.9(\pm 0.2) \cdot 10^{-16} \text{ cm}^3/\text{s} \text{ for } (\text{CH}_3)_2\text{S}$$

$$k_{24} = 1.8(\pm 0.2) \cdot 10^{-16} \text{ cm}^3/\text{s} \text{ for } (\text{CH}_3\text{S})_2$$

where the uncertainties indicate the width of the values obtained from the six runs.

It could be assumed that reaction 24 occurs via H-abstraction from the S-H bond, which is weaker than the C-H bond. This assumption would also be in line with the reduced rate constants observed in the case of dimethyl sulfide and dimethyl disulfide. However, if the hydrogen abstraction reaction CH₃SH + CH₃COO₂ → CH₃S + CH₃COO + OH, with CH₃COO further cleaved into CH₃ + CO₂, is included in the mechanism, then more methyl nitrate is produced in the simulation than experimentally observed and the *PAN* profile becomes too steep. If on the other hand the reaction is assumed to proceed via addition at the sulfur atom, then the

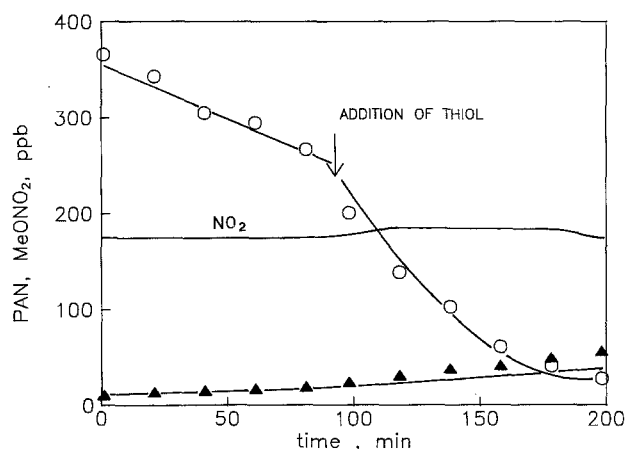


Fig. 2. Experimental and simulation results of *PAN* decay in the presence of added 500 ppm CH_3SH . Experimental points *PAN* O, CH_3ONO_2 ▲, simulations —

rate constants of CH_3COO_2 radicals like the other electrophilic radicals e. g. OH, NO_3 , would be expected to increase as substitution on the sulfur atom increases. This is not found to be the case in the CH_3COO_2 reactions studied here. It is also not found to be the case with the NO_3 reactions with CH_3SH , $\text{CH}_3\text{CH}_2\text{SH}$, $(\text{CH}_3)_2\text{S}$ and $(\text{CH}_3\text{S})_2$ as seen from their rate constants shown in Table 2, while it is partially found to be the case with the reactions of OH and the above sulfur compounds, with the apparent deviation being the reaction with $(\text{CH}_3)_2\text{S}$ which is considered to proceed via hydrogen abstraction.

In addition to *PAN* and CH_3ONO_2 the chromatograms obtained with the GC-ECD for each studied thiol showed another peak that increased with increasing reaction time, as shown in Fig. 3. The compounds that correspond to this peak for each of the three thiols used must contain the methyl, ethyl and butyl group as one can deduce from their increasing retention times of 0.90 min for CH_3SH , 1.96 min for $\text{C}_2\text{H}_5\text{SH}$, and 11.57 min for $\text{C}_4\text{H}_9\text{SH}$. The newly formed product must be strongly electron capturing because despite its coelution with the mother thiols, which have a relatively small response factor on the ECD, their chromatographic peak increased with the reaction time. Experiments carried out with pure NO_2 and CH_3SH showed the formation of a product with the same retention time as the one in the presence of *PAN*. Although pure *PAN* and CH_3SH formed the same product, this is probably due again to the reaction of CH_3SH with NO_2 which results from the thermal decay of *PAN*. Most probably this reaction product is of the type RSNO , where $R = \text{CH}_3$, CH_3CH_2 or $\text{CH}_3\text{CH}_2\text{CH}_2\text{CH}_2$. The dimethyl sulfide and dimethyl disulfide did not yield analogous products in agreement with their initial reactions with NO_2 proposed by Balla and Hecklen [14].

The main chemical destruction route of *PAN* is via its reaction with NO [reaction (18)]. The NO concentration in remote areas is a few ppt. The most abundant of the studied sulfur compounds is *DMS* averaging 100 ppt [20] in remote marine atmospheres. The difference in the concentration of NO and *DMS* cannot make up for the difference of five orders in the rate constants of reactions (18) and (24)

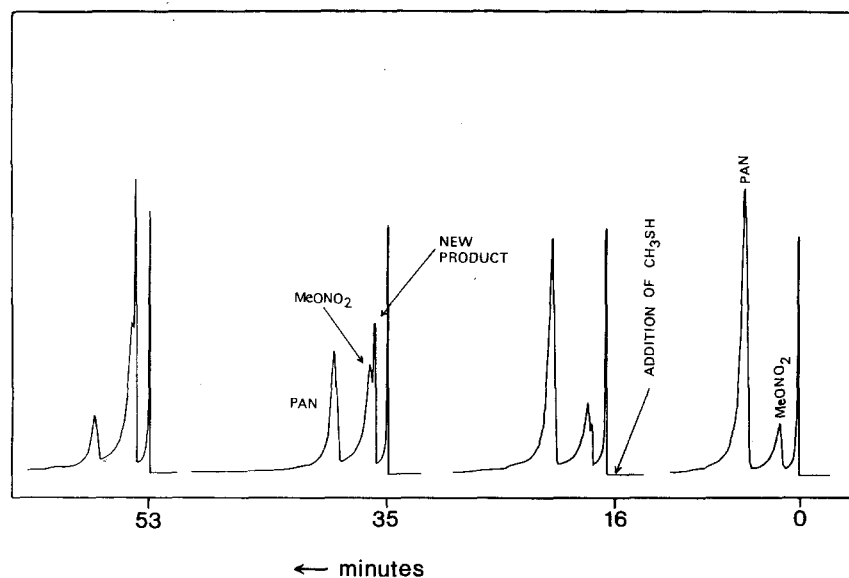


Fig. 3. Chromatograms showing the product variations vs. time for the reaction of methane thiol with *PAN* in the presence of NO_2

and we can thus conclude that the studied sulfur compounds would not be expected to affect the lifetime of *PAN* in clean atmospheres.

References

- [1] Pate C. T., Atkinson R., Pitts J. N. (1976) *J. Environ. Sci. Health, Environ. Sci. Eng. AII* (1) : 19
- [2] Cox R. A., Roffey M. J. (1977) *Environ. Sci. Technol.* **11**: 900
- [3] Schurath U., Vipprecht V. (1980) In: Versino B., Ott H. (eds.) *Physico-Chemical Behaviour of Atmospheric Pollutants*. Reidel D., Dordrecht, p. 157
- [4] Erickson D. J., Ghan S. J., Penner J. E. (1990) *J. Geophys. Res.* **95**: 7543
- [5] Gaffney J. S., Fajer R., Senum G. I. (1984) *Atmos. Environ.* **18**: 215
- [6] Roumelis N., Glavas S. (1992) *Monatsh. Chem.* **123**: 63
- [7] Atkinson R., Baulch D. L., Cox R. A., Hampson R. F. Jr., Kerr J. A., Troe J. (1989) *J. Phys. Chem. Ref. Data* **18**: 881
- [8] Moortgat G., Veyret B., Lesclaux R. (1989) *J. Phys. Chem.* **93**: 2362
- [9] Moortgat G. K., Veyret B., Lesclaux R. (1987) Cost 611, WP2 Meeting. Riso National Laboratory, Denmark, p. 24
- [10] Batt L., Rattray G. N. (1979) *Int. J. Chem. Kinet.* **11**: 1183
- [11] Yamada F., Slangie I., Gutman D. (1981) *Chem. Phys. Letts.* **83**: 409
- [12] Atkinson R., Lloyd A. C. (1984) *J. Phys. Chem. Ref. Data* **13**: 315
- [13] DeMore W. B., Sander S. P., Golden D. M., Molina M. J., Hampson R. F., Kurylo M. J., Howard C. J., Ravishankara A. R. (1990) *Chemical Kinetics and Photochemical Data for Use in Stratospheric Modeling* **9**
- [14] Balla R. J., Heicklen J. (1985) *J. Phys. Chem.* **89**: 4596
- [15] Balla R. J., Nelson H. H., McDonald J. R. (1986) *Chem. Phys.* **109**: 101
- [16] Black G., Jusinski L. E., Patrick R. (1988) *J. Phys. Chem.* **92**: 5972

- [17] McLeod H., Aschmann S. M., Atkinson R., Tuazon E. C., Winer A. M., Pitts J. N. Jr. (1986) *J. Geophys. Res.* **91**: 5338
- [18] Atkinson R. (1985) *Chem. Rev.* **85**: 69
- [19] Balla R. J., Heicklen J. (1984) *J. Phys. Chem.* **88**: 6314
- [20] Andreae M. O., Ferek R. J., Bermond F., Byrd K. P., Engstrom R. T., Hardin S., Houmère P. D., LeMarrec F. and Raemdonck H. (1985) *J. Geophys. Res.* **90**: 12891

Received August 8, 1991. Revised November 28, 1991. Accepted December 9, 1991